

## Short communication

## Hydroxyapatite layers prepared by sol–gel assisted electrostatic spray deposition

Byung-Hoon Kim<sup>a</sup>, Ju-Hyun Jeong<sup>a,b</sup>, Young-Sun Jeon<sup>a,b</sup>,  
Kyung-Ok Jeon<sup>a,b</sup>, Kyu-Seog Hwang<sup>b,\*</sup><sup>a</sup> Department of Materials Science & Engineering, Chonnam National University,  
300 Yongbong-dong, Buk-gu, Gwangju 500-757, South Korea<sup>b</sup> Department of Applied Optics and Institute of Photoelectronic Technology, Nambu University,  
864-1 Wolgye-dong, Gwangsan-gu, Gwangju 506-824, South Korea

Received 12 July 2005; received in revised form 27 July 2005; accepted 23 August 2005

Available online 12 October 2005

## Abstract

Hydroxyapatite (HAP) thin films were prepared by the sol–gel assisted electrostatic spray deposition (ESD) using calcium nitrate and phosphoric acid as starting materials. Methanol was used as solvent in the precursor solution. Final annealing was done at 500 °C for 30 min in air. Crystallinity, chemical structure, and surface morphology of the films were analyzed. Well-crystallized hydroxyapatite films were obtained by final annealing at 500 °C. Eighty degree celsius was the ideal substrate temperature for preparing smooth and dense hydroxyapatite films.

© 2005 Elsevier Ltd and Techna Group S.r.l. All rights reserved.

**Keywords:** Hydroxyapatite thin film; Calcium nitrate; Electrostatic spray deposition

## 1. Introduction

Calcium phosphate (CaP)-based bioceramics, mainly in the form of hydroxyapatite (HAP), have been in use in medicine and dentistry for the last 20 years. Applications include coating for orthopedic and dental implants, alveolar ridge augmentation, maxillofacial surgery, otolaryngology, and scaffolds for bone growth [1]. Nevertheless, poor mechanical properties prevent their use as load-bearing implants [2]. Thus, considerable research effort has been directed toward the development of calcium phosphate-based ceramic coatings on various substrates to achieve a strong, biocompatible material system for many prosthetic applications involving complex loadings arrangements. Several methods have been proposed for the production of CaP coatings including plasma spraying [3], RF magnetron sputtering [4], pulsed laser deposition [5], and electrodeposition [6]. However, the main problems of such coatings are the stoichiometry, the limitation of substrate shape, and precise control of the composition. Chemical solution deposition (CSD) such the sol–gel process [7,8] has been

proved promising for thin films applicable on a variety of substrates, of low cost and a precise control of chemical composition.

Recently, a novel and cost-effective deposition method called electrostatic spray deposition (ESD) has been used to prepare thin films of oxidic materials [9,10]. A liquid flowing through a capillary nozzle can be subjected to a high voltage to produce a spray. This process can be carried out in several modes, and the cone–jet mode, in which the spray emanates from the tip of a liquid cone, can produce near-monodispersed droplets [10].

In this work, we combine these two techniques, sol–gel process and ESD, to prepare high quality HAP thin films.

## 2. Experimental

Calcium nitrate ( $\text{Ca}(\text{NO}_3)_2 \cdot 2\text{H}_2\text{O}$ , Merck, Germany), and phosphoric acid ( $\text{H}_3\text{PO}_4$ , Merck, Germany) were used as reactants for the preparation of CaP thin films. The sol was diluted with methanol to adjust the concentration [metal (Ca + P):MeOH = 5:95 mol%] and viscosity for preparing thin films by ESD. The molar ratio of metals in the precursor solution was set as Ca:P = 1.67:1. Fig. 1 shows a schematic diagram of the ESD system used in this work. A stainless steel

\* Corresponding author. Tel.: +82 62 9700110; fax: +82 62 9700288.

E-mail address: khwang@nambu.ac.kr (K.-S. Hwang).

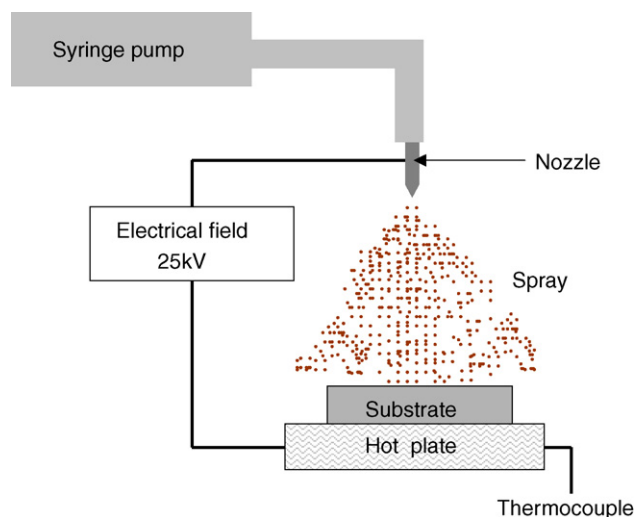


Fig. 1. Schematic diagram of ESD setup.

Table 1

List of the different coating parameters and the results

Parameters		Film formation
Applied voltage (kV)	Heating temperature (°C)	
5	50	×
5	80	×
5	120	×
15	50	×
15	80	△
15	120	×
25	50	×
25	80	○
25	120	×

(×): bad; (△): common; and (○) good.

A large number of solvents for pyrolysis and vapor deposition of coatings has been experimented [11]. It was found that methanol is capable of creating more droplets for deposition near the vaporizing zone than other commonly used solvents for vapor deposition. According to these authors, this depends on the saturation of vapor pressure of the solvent  $P_s$ , the viscosity of the solvent  $\eta$  and the surface tension of the solvent  $\tau$ . The proportionality factor  $\beta$  controls the formation of droplets. This factor is given by

$$\beta = \frac{P_s}{\eta\tau} \quad (1)$$

Compared to methanol, solvents including water, butanol, and higher alcohols give low  $\beta$  values [9]. In this work, the solvent, methanol having a high  $\beta$  value, plays a role in good formation of the film.

It can be seen that the HAP film deposited at 50 °C (Table 1 and Fig. 2a) is cracked. The formation of the cracked layer clearly indicates that the solvent in the spray droplets did not evaporate completely before reaching the substrate surface. This morphology is always found to be present if the deposition temperature is too low.

Indeed, when the thickness of the film reaches a critical value, cracks will occur due to the large vaporization of organics in the coatings deposited at the lower deposition temperature. On the other hand, increase in deposition temperature to 150 °C leads to agglomeration on the top of a dense bottom layer. An increasing number of particles is found on the surface of the film as shown in Fig. 2c, due to the greater extent of evaporation of the solvent during the transport of aerosol droplets from the nozzle to the substrate. Therefore, heating temperature during deposition is a critical parameter for the morphology of the film. In order to prepare dense thin films as shown in Fig. 2b, the ideal condition during deposition is that the evaporation rate of the solvent is equal to the deposition rate of the droplets [12]. From the film deposited at 80 °C, a crack-free and dense structure was obtained.

Eighty degree celsius appears to be the ideal substrate temperature for preparing smooth and dense HAP films. This deposition temperature approaches the boiling point of the methanol solvent, which is 84 °C.

needle (0.1 mm and 0.23 mm inner and outer diameter, respectively) was connected to a syringe pump (KD100, KD Scientific Inc., PA, USA) using a silicon rubber tube. The flow rate of the precursor solution was kept at 10 mL/60 min. In order to obtain a stable cone-jet mode of electrostatic atomization, a high voltage (5, 15 and 25 kV) was applied between the needle tip and ground electrode by using a dc power supply (SHV120-30K-RD, Converttech Co. Ltd., South Korea). Si wafers cleaned in a  $H_2O_2$  solution, and rinsed in methanol were used as substrate. Si was selected to facilitate use of the analytical techniques chosen for this study. Si substrates on the ground electrode were heated at 50–120 °C to vaporize the organic compound in the precursor solution during spraying. The precursor solution was pumped for 5 min through the nozzle placed 15 cm above the substrates. The as-deposited films were placed on an alumina boat and heated to 500 °C for 30 min in a tube furnace in the presence of air (flow rate approximately 150–200 mL/min).

The viscosity of the coating solution, 4–5 cP, was measured with a Bookfield cone-plate viscometer (Model DV-II). The crystal structure of the finally annealed films was characterized by X-ray diffraction (XRD, D-Max-1200, Rigaku Co., Japan) using Cu K $\alpha$  radiation ( $\lambda = 1.54056 \text{ \AA}$ ) generated at 40 kV and 30 mA in the  $20^\circ < 2\theta < 50^\circ$  range. The Fourier transform infrared (FTIR, FTS-60, BIO-RAD Digilab Co., USA) spectroscopy was performed to analyze the chemical structure of the films. The morphology of the films was examined by means of a field emission-scanning electron microscope (FE-SEM, S-4700, Hitachi Co., Japan).

### 3. Results and discussion

Table 1 collects the coating parameters and the quality of the films after deposition. Different from conventional spray processes, the spray in an ESD process consists of mainly charged droplets, which may be nanosized when generated. Furthermore, a pure or mixed alcohol is usually used as solvent [10].

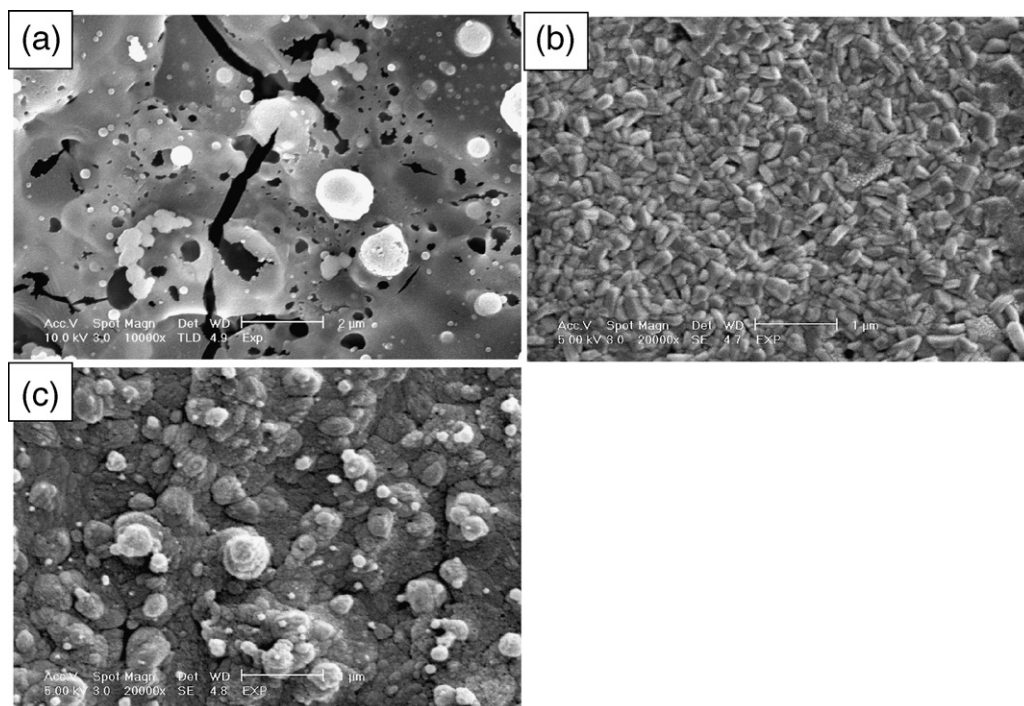


Fig. 2. FE-SEM image of the HAP films deposited at: 50 °C (a); 80 °C (b); and 120 °C (c) followed by annealing at 500 °C.

The deposition mechanism of the ESD method used in this work is similar to the synthesis mechanism occurring a sol–gel process. In the case of the sol–gel process, metal ions mixed at atomic scale exist in a sol precursor solution and then a dried gel precursor decomposes and crystallizes simultaneously through pyrolysis [13]. The ESD method usually atomizes a precursor solution containing metal ions mixed at atomic scale into an aerosol, which is then directed to a heated substrate. Desired films are formed on the heated substrate on further annealing by simultaneous decomposition of the precursor solution and synthesis of the metal oxide. Conclusively, mixing the two methods make possible a better mixing of the elements and, therefore, a better reactivity of the mixture.

In this work, the formation of dense and crack-free HAP thin films is a clear indication that the methanol solvent in the spray droplets has not been evaporated completely when reaching the substrate surface. The solution droplets may spread on the substrate surface and form such a dense layer.

Fig. 3 shows the XRD pattern of the films deposited at 25 kV and at 80 °C, followed by annealing at 500 °C. Thin films before annealing possess an amorphous structure, not shown here. The HAP,  $\text{Ca}_5(\text{PO}_4)_3(\text{OH})$ , structure (JC-PDS File 24-0033) started to become visible with peaks corresponding to the (0 0 2), (2 1 1), (1 1 2) and (3 0 0) reflections at around  $2\theta = 25^\circ$ – $26^\circ$ ,  $31.5^\circ$ – $31.8^\circ$ ,  $32^\circ$ – $32.5^\circ$  and  $32.5^\circ$ – $33^\circ$ . This implies that the final annealing process at 500 °C is effective in transforming the amorphous phase to the HAP crystalline phase.

In order to confirm the chemical structure of the annealed films, FTIR analysis were performed, as shown in Fig. 4. FTIR measurement showed distinct  $\nu_3$  (at around  $1110$ – $1120\text{ cm}^{-1}$ ),  $\nu_2$  (at around  $900\text{ cm}^{-1}$ ), and  $\nu_4$  (at around  $620\text{ cm}^{-1}$ )

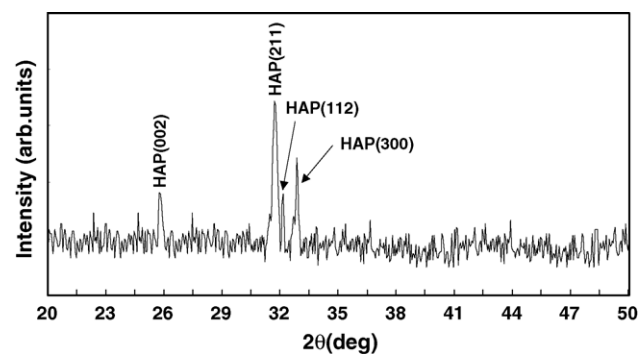


Fig. 3. XRD pattern of the HAP film deposited at 80 °C, followed by annealing at 500 °C.

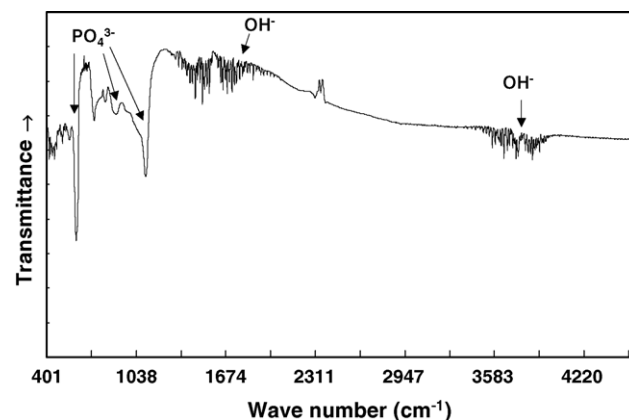


Fig. 4. FTIR spectra of the HAP film deposited at 80 °C, followed by annealing at 500 °C.

phosphate ( $\text{PO}_4^{3-}$ ) spectral bands. Films showed peaks at  $1700\text{ cm}^{-1}$  and  $3600\text{--}3700\text{ cm}^{-1}$  which is due to water absorbed from the surface. The appearance of three distinct peaks at  $1110\text{--}1120\text{ cm}^{-1}$ ,  $900\text{ cm}^{-1}$ ,  $620\text{ cm}^{-1}$  has been observed as an evidence of HAP [1]. The group centered at about  $1110\text{--}1120\text{ cm}^{-1}$  is due to the stretching mode of P–O bonds. Thus, the sharpness of this peak can be correlated with a high degree of crystallinity of the HAP.

#### 4. Conclusions

HAP thin films via sol–gel assisted ESD process have been obtained. The amorphous as-deposited films transformed to HAP films at  $500^\circ\text{C}$ . Surface morphology of the HAP films deposited at  $80^\circ\text{C}$  showed a crack-free and dense structure, while the surface of the film deposited at lower or higher temperature than boiling point of methanol exhibited cracks and agglomeration. It is found that  $80^\circ\text{C}$ , which is similar to the boiling point of methanol, is the ideal temperature during deposition for preparing smooth and dense HAP films.

#### References

- [1] K.S. Hwang, J.E. Song, B.A. Kang, Y.J. Park, *Surf. Coat. Technol.* 123 (2000) 252–255.
- [2] C.S. Chai, B. Ben-Nissan, *J. Mater. Sci.: Mater. Med.* 10 (1999) 465–469.
- [3] S.W. Ha, R. reber, K.L. Wckert, M. Petimermet, J. Mayer, E. Wintermantel, C. Baerlocher, H. Gruner, *J. Am. Ceram. Soc.* 81 (1) (1998) 81–88.
- [4] K. van Dijk, H.G. Schaeken, J.C.G. Wolke, C.H.M. Marée, F.H.P.M. Habraken, J. Verhoeven, J.A. Jansen, *J. Biomed. Mater. Res.* 29 (1995) 269–276.
- [5] B.E. Tucker, C.M. Cottell, R.C.Y. Auyeung, M. Spector, G.H. Nancollas, *Biomaterials* 17 (1996) 631–637.
- [6] H. Dasarathy, C. Riley, H.D. Coble, W.R. Lacefield, G. Maybee, *J. Biomed. Mater. Res.* 31 (1996) 81–89.
- [7] K. Hwang, Y. Lim, *Surf. Coat. Technol.* 115 (1999) 172–175.
- [8] Y. Lim, Y. Park, Y. Yun, K. Hwang, *Ceram. Int.* 28 (2002) 37–41.
- [9] R. Chandrasekhar, K.L. Choy, *J. Cryst. Growth* 231 (2001) 215–221.
- [10] C.H. Chen, K. Nord-Varhaug, J. Schoonman, *J. Mater. Synth. Process.* 4 (3) (1996) 189–194.
- [11] A. Smith, J.M. Laurent, D.S. Smith, J.P. Bonnet, R. Rodriguez-clemente, *Thin Solid Films* 266 (1995) 20–30.
- [12] H. Huang, X. Yao, X. Wu, M. Wang, L. Zhang, *Microelectron. Eng.* 66 (2003) 688–694.
- [13] W. Yoon, S. Ban, K. Lee, K. Kim, M. Kim, J. Lee, *J. Power Sources* 97–98 (2001) 282–286.